INNSPUB

Journal of Biodiversity and Environmental Sciences (JBES)
ISSN: 2220-6663 (Print) 2222-3045 (Online)
Vol. 22, No. 1, p. 50-65, 2023
http://www.innspub.net

RESEARCH PAPER OPEN ACCESS

Adsorption of dye from aqueous solutions by orange peel with Chitosan nanocomposite: Equilibrium studies

SP. Manobala[1], S. Amutha[1], G. Sabeena[*1], E. Amutha[1], M. Sharmila[1], S. Rajaduraipandian[2]

[1]*Sri Paramakalyani Centre of Excellence in Environmental Sciences, Manonmaniam Sundaranar University, Alwarkurichi, India*

[2]*Sri Paramakalyani College, Manonmaniam Sundaranar University, Alwarkurichi, India*

Article published on January 11, 2023

Key words: Adsorption, Methylene blue, Orange peel, Chitosan, Chitosan nanoparticle, Isotherms

Abstract

This research focused on the development of adsorbents based on cheap, abundant, and locally available agricultural wastes in Tamil Nadu to adsorb dye from an aqueous solution. The goal of this study was to explore if chitosan-modified orange peel could be utilized as an adsorbent to remove colours from wastewater and if it could be employed as a traditional wastewater treatment approach in the textile sector. Using agricultural peel in decolouration technology has a lot of potential in terms of efficiency, cost-effectiveness, and environmental friendliness. Super nanocomposite is made from orange peel waste combined with chitosan nanoparticles. The purpose of this batch adsorption experiment was to determine the effects of adsorbent dosages, pH, and temperature on dye adsorption from wastewater. The experiment showed that the maximum amount of dye adsorbed was 53.3mg/g at pH 6.9 with a Temperature (of 60° C) and the adsorbent dose amount of adsorbent was 1.0g/L. The Langmuir adsorption isotherm model was used to investigate the equilibrium adsorption behaviour. The usage of orange peel with Nanocomposite as an adsorbent for the adsorption of methylene blue dye from solutions was demonstrated in this work. The functional groups and chemical compounds found in orange peels, chitosan, chitosan orange peel, chitosan nanoparticle, and chitosan nanoparticle with orange peel waste were identified using FTIR, TGA, and SEM techniques. Different types of Langmuir I, Langmuir II, Langmuir III, Langmuir IV, and the Freundlich model as adsorption isotherm models were investigated.

***Corresponding Author:** G. Sabeena ✉ gannadurai@msuniv.ac.in

Introduction

Annual production of textile dyes is estimated to be over 8×10^5 tonnes of which 10% are discharged as effluents (Zollinger, 1987). The release of these dyes in the water stream is aesthetically undesirable and has a serious environmental impact. Due to their intense colour, they reduce sunlight transmission into water hence affecting aquatic plants, which ultimately disturbs the aquatic ecosystem; in addition, they are toxic to humans also. The printing and textile industry mainly contribute to the discharge of dye effluent and the governments of different countries have enacted strict rules controlling the discharge of waste. To minimize pollution, manufacturers and government officials are seeking for solutions to tackle the problem efficiently. People are looking for a system that can remove most of the colour and generate reusable water from the effluent. Synthetic dyes are resistant to biological treatment and can produce harmful by-products during hydrolysis, oxidation, or other chemical reactions taking place in the wastewater (Li *et al.,* 2007). Traditional techniques such as carbon adsorption and coagulation by chemical agents are non-destructive and simply transfer the contaminant from water to another phase. A low-cost complete mineralization process for the azo dyes would find extensive use for the treatment of large volumes of wastewater generated from the textile industry. There are several methods for dye removal which include chemical coagulation, flocculation, chemical oxidation, photochemical degradation, membrane filtration, and aerobic and anaerobic biological degradation but all of these methods suffer from one or other limitations, and none of them were successful in completely removing the colour from wastewater. Dyes can be effectively removed by the adsorption process; in which dissolved dye compounds attach themselves to the surface of adsorbents (Slokar *et al.,* 1997; Neil *et* al., 1999; Dizge *et al.,* 2008).

The adsorption process/technique is widely used in the removal of contaminants from wastewater. Liquid–solid adsorption operations are concerned with the ability of certain solids to preferentially concentrate specific substances from solution onto their surfaces (Chen *et al.,* 2007). This promoted search for an alternative cost-effective adsorbent. Recently different low-cost adsorbents including some industrial and agricultural wastes (Gordan McKay *et al.,* 1985; Namasivayam *et al.,* 2001; Netpradit *et al.,*2003; Gordan McKay *et al.,* 1980; Namasivayam *et al.,* 1992; Namasivayam *et al.,* 1996; McKay *et al.,* 1986) such as fly ash, fuller's earth, waste red mud, bentonite clay, metal hydroxide sludge, peat, pith, cotton waste, rice husk, teakwood bark, etc. have been used but their effectiveness is limited and inferior to that of activated carbon. Adsorption has been extensively used in industrial processes for either separation or purification. Most conventional adsorption plants use activated carbon, which is an expensive material. Besides, there is growing interest in searching for cheaper sources as low-cost adsorbent materials for the adsorption of dyes such as coir pith, sugar cane dust, sawdust, and activated carbon fibers (Janos *et al.,* 2003; Viraraghavan *et al.,* 1999; Acemioglu *et al.,* 2004; Mohan *et al.,* 2002; Al-Qodah, 2000) industrial solid wastes: fly ash, shale oil ash, and so on.

Currently, traditional solutions for orange peel waste management (landfilling, composting, pectin extraction, animal feeding) are not economically attractive, since they present many drawbacks. Traditional handling techniques are either not economically attractive or discouraged by European policy. As an alternative to these technologies, others aimed at recovering energy and resources are currently receiving increasing attention. The consequential life cycle assessment adopted in this work compares the environmental performance of ten orange peel waste management scenarios (Yoo *et al.,* 2011) orange peel waste use adsorption studies for the removal of dyes from Industrial Effluents. Chitosan is a polysaccharide that is a chitin chemical derivative. Chitin has been isolated from mollusks, crabs, prawns, shrimp, crayfish, and lobsters, among other invertebrates. Chitins are polymers made up of a 2-acetamido-2-deoxy-D-glucose disaccharide connected by a (1-4) bond. Deacetylation of chitin with sufficient

acetyl glucosamine units revealed chitosan. Chitosan has thus found its way into a variety of applications, including adsorption, tissue regeneration, drug delivery, biosensors, and wound dressings.

The adsorption ability of methylene blue dye utilizing orange peel with chitosan nanocomposite as an adsorbent from aqueous solutions was investigated in this study. Under equilibrium settings, the effects of doses, pH, and temperature on the orange peel with chitosan nanocomposite were examined.

The adsorption equilibrium data are used to evaluate the rate-limiting step of methylene blue adsorptions onto orange peel with chitosan nanocomposite. The experimental data were computed using both the Langmuir (Different Types) and Freundlich adsorption isotherms.

Materials and methods

Materials

The following chemicals were of analytical grades Chitosan powder, Acetic acid glacial (CH_3COOH) 100% GR (Merck), Sodium Tripolyphosphate ($Na_5O_{10}P_3$), and double distilled water. Analytical grade Methylthionium chloride, commonly called Methylene blue, is a salt used as a dye and as a medication. Methylene blue is a thiazine dye CI: 52015. It works by converting the ferric iron in haemoglobin to ferrous iron. Chemical formula $C_{16}H_{18}ClN_3S$, Molar mass 319.85 g/mol was purchased from Merck.

Orange peel

Orange peel will be obtained from a Tirunelveli fruit market. They threw away a lot of orange peels. These discarded peels can be used to remove colours from wastewater as an adsorbent. To remove dust particles and water-soluble contaminants, the peels were first cleansed with distilled water. The peels will be rinsed numerous times to eliminate any dirt or moisture that has adhered to them. They will be dried for 48 hours at 40° C before being ball-milled to produce a uniform geometrical size for use. Finally, the grounded peels were packed in an airtight container and labeled.

Synthesis of orange peel with chitosan composites

5g of chitosan was dissolved in 5% acetic acid and stirred for 30 minutes to dissolve the chitosan and 5g of orange peel waste was added to the solution. The reaction was kept for about 2- 4 hours with constant stirring. The mixture was before calcinated at 200°C. The orange peel with chitosan composite was synthesized.

Synthesis of Chitosan nanoparticle

Ionic gelation was used to create chitosan nanoparticles from chitosan 5g of chitosan was dissolved in 5% acetic acid and stirred for 30 minutes to dissolve the chitosan. Sodium tripolyphosphate (STPP) was used as a cross-linking agent and was added dropwise. As a result, chitosan becomes a nanoparticle. The magnetic stirrer was used to mix the mixture at the same time. After 12 hours of stirring at room temperature, the solution was centrifuged for 30 minutes and kept warm in a hot air oven. This is what causes the powder to form.

Synthesis of orange peel with chitosan nanocomposites

5g of Chitosan nanoparticle was mixed with 100mL of distilled water, and 5g of orange peel waste was added to the solution. The reaction kept going for about 2-4 hours. It was then centrifuged for 30 minutes and dried in a hot air oven at 100°C. The powder was ground with a mortar and pestle before being calcined at 200°C. The orange peel with chitosan nanocomposite was synthesized.

Batch adsorption experiments

Adsorption tests were conducted in a batch method with 0.1 of the chitosan nanoparticles with orange peel nanocomposite suspended in water. The orange peel with chitosan nanocomposite was combined with 100mL of Methylene blue dye solution (20-100mg/L) in an Erlenmeyer flask at different dosages (1.0, 2.0, and 3.0g/L), pH (5.3, 6.9, 7.6), and temperatures (30°C, 45°C, and 60°C). On a water shaker thermostat, the mixture was equilibrated for 24 hours at 60 rpm. Using a UV/ Vis Spectrometer to record the absorbance of the supernatant at a max of 665 nm, the residual concentrations of the adsorbate were determined. Calculating the adsorption capacity under a variety of parameter settings was used to explore the adsorption isotherms.

A mass balance equation was used, to find the amount of dye adsorbed in each flask which was determined by the equation,

$$q_e = \frac{C_I - C_F}{m} \times v \qquad (1)$$

Where, qe = Adsorbed amount (mg/g); C_I = initial concentration of (mg/L); C_F = Final concentration of (mg/L); V = Volume of adsorbate; m = Mass of used.

Table 1. Isotherms and their linear forms.

Isotherm	Linear Regression	Plot
Langmuir Isotherm Type 1 (Eq-2)	$C_e / q_e = (1/K_L q_m) + (C_e / q_m)$	$C_e / q_e .vs. C_e$
Langmuir Isotherm Type 2	$1 / q_e = (1 / q_m) + (1 / K_L q_m C_e)$	$1 / q_e .vs. 1 / C_e$
Langmuir Isotherm Type 3	$q_e = q_m - (q_e / K_L C_e)$	$q_e .vs. q_e / C_e$
Langmuir Isotherm Type 4	$q_e / C_e = K_L q_m - K_L q_e$	$q_e / C_e .vs. q_e$
Freundlich Isotherm (Eq-3)	$Log(C_e) = Log(K_F) + 1/n Log(C_e)$	$Log(q_e) .vs. Log(C_e)$

FT-IR spectrophotometry

The functional groups on the peels were studied using FT-IR spectrophotometry in the range of 4000 to 500cm^{-1} fig.1.The broadband was observed at 2854 - 3427cm^{-1} for all orange peel, Chitosan, Chitosan with Orange peel, chitosan nanoparticle and chitosan nanoparticle with orange peel nanocomposite matches the O-H stretching frequency, it can originate from intermolecular hydrogen bonds linking the compounds and alcohols, phenols and carboxylic acids.

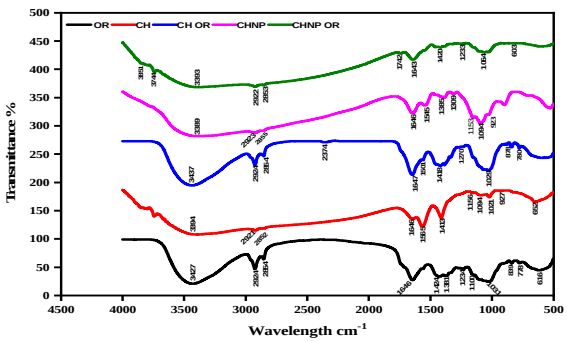

Fig. 1. FTIR curves of the Orange Peel, Chitosan with orange peel, Chitosan Nanoparticle, and Chitosan Nanoparticle with Orange Peel Nanocomposite.

Broad and intense absorption peaks at 3427cm^{-1} in the spectrum of the orange peel correspond to the –OH stretching vibrations of cellulose, pectin, hemicellulose, and lignin. The C–H stretching vibrations of the methyl, methylene, and methoxy groups have a peak at 2922cm^{-1}. The strong adsorption of about 1031- 616cm^{-1} under the frequency of functional groups lasted aromatic C-H and C=O groups linked compounds aldehydes, ketones, esters, amides, and carboxylic acids. The absorption bands at 1741cm^{-1} and 1622cm^{-1} represented C=O stretching present in hemicelluloses (Arthanarieswaran *et al.,* 2015) and -C=C- stretching respectively. The 1521cm^{-1} arises due to the C=C ring stretching (Aromatic group). The peak was observed at 1438cm^{-1} due to carbonyl stretching raise in lignin (Li *et al.,* 2019; Li *et al.,* 2019; Sung *et al.,* 2002). The bands in the fingerprint region, 1016cm^{-1} clarified the C-O-C vibrational stretching of polysaccharides (Ashok *et al.,* 2018) and 838cm^{-1} confirming the presence of glucosidic (β) linkages between hemicelluloses and cellulose sugar units (Arthanarieswaran *et al.,* 2015). The C- OH bending in cellulose was observed through a peak at 598cm^{-1} (Santhanam *et al.,* 2016; Rahman *et al.,* 2015). The peak at 1031cm^{-1} clearly shows the presence of the C-O group in the carboxylic and alcoholic. Peaks observed at around 2854cm^{-1} can be attributed to the C-H stretching frequency. The relatively wide central peak of about 1646cm-1 stems from the extension of the C-C aromatic ring (Mafra *et al.,* 2013). The adsorption peaks in the range of 1000-1500cm^{-1} can be considered for angular deformation in the bonding plane of C-H aromatic rings. In addition, consecutive peaks in the 3427-4000cm^{-1} range may be assigned to the N-H bond (Arulmozhi *et al.,* 2013). It can be seen that the surface of sorbents contains functional groups such as hydroxyl and carboxyl groups necessary for the adsorption of dye molecules (Sugumaran *et al.,* 2012; Chandra *et al.,* 2009).

Thermogravimetric Analysis (TGA)

TGA analysis is used to determine the thermal stability of a material based on weight loss as temperature rises.

The TGA thermograms of Orange Peel, Chitosan with orange peel, Chitosan nanoparticles, and Chitosan nanoparticles with Orange Peel Nanocomposite were shown in fig.2. Thermal deterioration was detected in three phases in both powders, as shown by TGA curves. Although the stages mentioned above are mainly characterized by the degradation of hemicellulose and cellulose, the simultaneous decomposition of lignin is also present in that temperature range; after 200 °C, there is a prolonged weight loss that can be attributed to the last stage of lignin degradation (Lopez-Velazquez *et al.,* 2013). A slow weight loss from 160 - 400 °C may be due to the decomposition of the low molecular weight chitosan followed by a more obvious weight loss from 210 - 380 °C, due to a complex process that includes dehydration of the chitosan anhydroglucosidic ring (Gomathi *et al.,* 1794-1806).

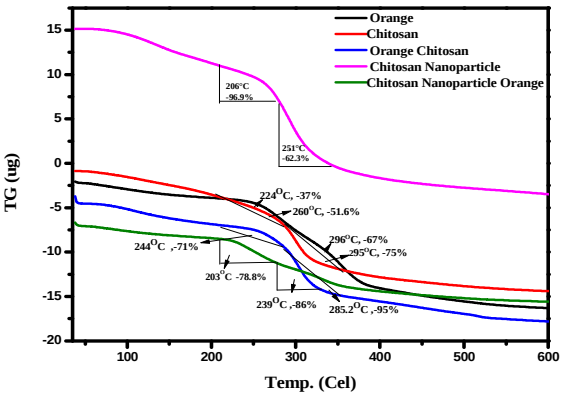

Fig. 2. TGA curves of the Orange Peel, Chitosan with orange peel, Chitosan Nanoparticle, and Chitosan Nanoparticle with Orange Peel Nanocomposite.

At weight loss was for Orange Peel, Chitosan with orange peel, Chitosan Nanoparticle, and Chitosan Nanoparticle with Orange Peel Nanocomposite for Orange Peel, 224°C-37%, 260°C-51.6%t for Chitosan, 244°C-71.0 %, 282.2°C-95% for Chitosan with Orange Peel, 206°C-96 (Tverdokhlebov *et al.,* 2012). Because of the full degradation of adsorbents, the larger mass reduction of Orange Peel, Chitosan with orange peel, Chitosan Nanoparticle, and Chitosan Nanoparticle with Orange Peel Nanocomposite was seen between 100°C and 600°C (Khan *et al.,* 2015). Due to the inclusion of thermally stable chitosan nanoparticles, the point of inflection in orange peel, chitosan differs from chitosan with orange peel, chitosan nanoparticle with orange peel nanocomposite. Due to the inclusion of thermally stable chitosan nanoparticles, the point of inflection in orange peel, chitosan differs from chitosan with orange peel, chitosan nanoparticle with orange peel nanocomposite. Orange Peel, Chitosan with orange peel, Chitosan Nanoparticle, and Chitosan Nanoparticle with Orange Peel Nanocomposite are all thermally stable up to 360°C, whereas Chitosan nanoparticle is thermally stable up to 600°C. The incorporation of high thermal withstanding capacity chitosan Nanoparticles accounts for the greater residual masses of chitosan with orange peel.

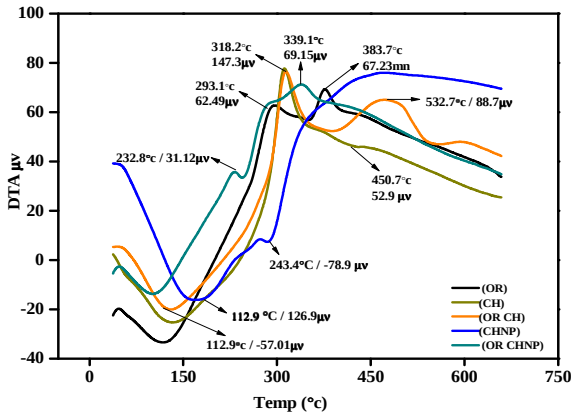

Fig. 3. DTA curves of the Orange Peel, Chitosan with orange peel, Chitosan Nanoparticle, and Chitosan Nanoparticle with Orange Peel Nanocomposite.

For swapped Orange Peel, Chitosan with Orange Peel, Chitosan Nanoparticle, and Chitosan Nanoparticle with Orange Peel Nanocomposite, the thermal curves in the Room Temperature (RT) range are displayed in fig.3. Two phases are visible in the thermal curves overall structure: one in the temperature range of RT to 150°C and the other in that of 150°C to 600° C. The dehydroxylation of the Cellulose and carboxyl methylcellulose structure, which occasionally occurs dissociated in two, has been attributed to the first step in Orange Peel, Chitosan with orange peel, Chitosan Nanoparticle, and Chitosan Nanoparticle with Orange Peel Nanocomposite. This step is visible in the corresponding DTG fig.4 at 200°C and 400°C.

The endothermic phenomena span from RT to 150°C according to the DTA curve for Orange Peel, Chitosan with Orange Peel, Chitosan Nanoparticle, and Chitosan Nanoparticle with Orange Peel Nanocomposite fig.3. These temperature ranges cause both physisorbed water that has been adsorbed on the clay's exterior surface and water from the interlamellar space to evaporate. The second stage involves a multi-step dehydroxylation between 250 and 400°C for the Orange Peel, Chitosan with Orange Peel, Chitosan Nanoparticle, and Chitosan Nanoparticle with Orange Peel Nanocomposite (Sun Kou *et al.,* 1998).

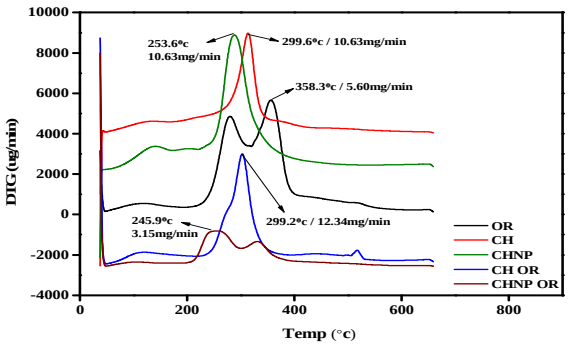

Fig. 4. DTG curves of the Orange Peel, Chitosan with orange peel, Chitosan Nanoparticle, and Chitosan Nanoparticle with Orange Peel Nanocomposite.

The DTA curves for orange peel, chitosan with orange peel, chitosan nanoparticle, and chitosan nanoparticle with orange peel nanocomposite do not deviate significantly from the parent material; however, one additional feature of the curve is the loss of definition of the peaks at about 300°C and 450°C, which is visible in the case of orange peel, chitosan with orange peel, chitosan nanoparticle, and These peaks in the parent clay were linked to interlamellar water loss and dehydroxylation from various settings.

Scanning Electron Microscopy

The result of the SEM analysis is shown in fig.5 (A)–(E). It can be seen from fig.5(A)–(E) that orange peel, Chitosan Nanoparticle, and Chitosan Nanoparticle with Orange Peel Nanocomposite surface are rippled paper-like smooth, compact sheet before chemical modification. The morphology of chitosan with and without orange peel was shown by SEM pictures of the surface and sectional profile. There weren't many grains or porous structures to be found.Orange peel chitosan has a flat, homogeneous shape with uniformly distributed pores and a porous morphology.

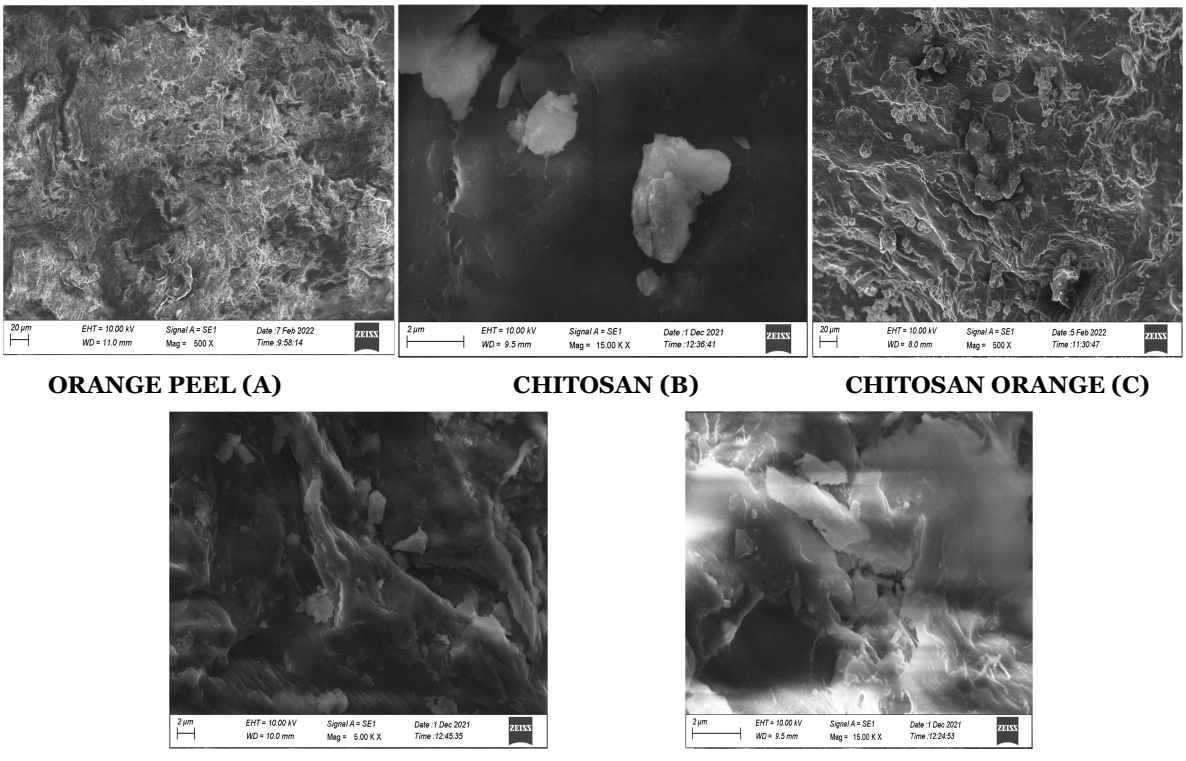

Fig.5. SEM curves of the Orange Peel, Chitosan with orange peel, Chitosan Nanoparticle, and Chitosan Nanoparticle with Orange Peel Nanocomposite.

In comparison to chitosan, the orange peel-chitosan combination produced noticeable oil droplet forms (Sugumar *et al.*, 2015; Yunus Alparslan *et al.,* 2017; Saini *et al.,* 2018; Hafsa *et al.,* 2016) found that adding essential oils resulted in a heterogeneous structure with oil droplets entrapped in the continuous polysaccharide network. Fig.5 (A)–(E) shows an SEM picture of chitosan with orange nanocomposite powder, revealing the porous structure that could give more dye adsorption sites.

Effects of amount of adsorbent

A 1000mg/L methylene dye solution was produced by weighing 1g/L and dissolving it in distilled water in a 250-mL standard flask. Working standards containing various concentrations of cadmium ions (25–100mg/L) were produced from the stock solution in 250-mL standard flasks and marked. Fig.6 shows how the adsorption capacity improved as the adsorbent dosage was increased.

The waste removal percentage has increased from 35mg/g to 49mg/g, and the adsorbent dosages have been increased from 1.0 g/L to 3.0 g/L for a 100mL solution. As a result of the increased mass of adsorbent, more surface area was created. As a result, the overall number of sites grows. Furthermore, the figure reveals that the maximum adsorption increases as the dosage are increased above 1.0g.

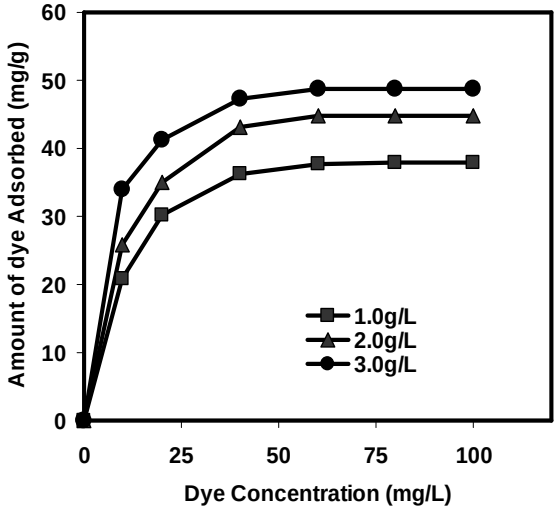

Fig. 6. Effect of specific dye uptake at different adsorbent dosages with methylene dye concentration.

Effect of pH

The adsorption of colours by chitosan nanoparticles with orange peel Nanocomposite is greatly influenced by the pH of the solution. The effect of pH on methylene blue adsorption is seen in fig.7. The percentage elimination reduced from 87 to 63 when the dye solution's starting pH was adjusted from 2 to 11. The highest amount of dye adsorbed dropped from 15 to 40mg/g when the pH increased from 5.3 to 6.9. There was a small decrease in dye adsorption as the pH was increased to 6.9. The presence of an excess of OH^+ ions competing with the dye anions for adsorption sites results in lower methylene blue adsorption at alkaline pH. The number of positively charged sites on the adsorbent decreases as the pH of the system rises, and the amount of positively charged surface sites on the adsorbent favours anions adsorption due to electrostatic attraction. The dye adsorption capability of chitosan nanoparticles containing orange peel was found to be more effective at an average pH. At pH 6.9, the best adsorption capacity was found. At lower pH, the peels functional oxidized groups are encouraged, making the active site of the chitosan nanoparticle-containing orange peel for dye-binding less available. As a result, the efficiency of adsorption falls. The adsorption of Acid Violet by biogas residual slurry (Namasivayam *et al.,* 1994) and banana pith (Namasivayam *et al.,* 1994) produced similar results (Namasivayam *et al.,* 2001). According to the classification of maximum adsorption ability for monolayers, chitosan nanoparticles containing orange peel have a high q_m value, indicating that they have a stronger adsorption potential.

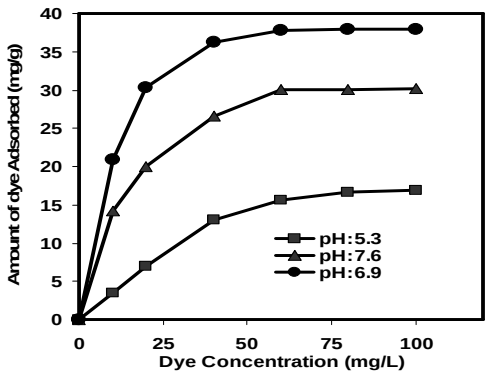

Fig. 7. Effect of specific dye uptake at different pH with methylene dye concentration.

Effect of temperature

In this experiment, 25mL of 100mg/L methylene blue dye solution was agitated with 1.0 g powdered chitosan nanoparticle with orange peel nanocomposite at pH 6.9 and temperatures ranging from 30 to 60°C as shown in fig.8. With the help of an orbital shaker, the mixture was regularly shaken. After filtering the solution, UV-Visible Spectroscopy was used to identify the liquid portion. The increased mobility of the large methylene blue dye ion, as well as a swelling action within the internal structure of the chitosan nanoparticle with orange peel, allows the large dye molecule to penetrate further (Namasivayam *et al., et al.,* 2001; Namasivayam *et al., et al.,* 2002; Ho *et al.,* 1999). As a result, adsorption capacity should be mostly determined by chemical interactions between functional groups on the adsorbent surface and the adsorbate and should increase as temperature rises. The current study's findings on methylene blue dye adsorption at higher temperatures are similar to those of (Namasivayam *et al., et al.,* 2001; Namasivayam *et al., et al.,* 2002; Ho *et al.,* 1999). At a pH of 6.9, the maximum % removal of 55.2 g/L was recorded for methylene blue dye at a concentration of 40mg/L. In acidic solutions, methylene blue dye uptake is substantially higher than in neutral and alkaline solutions.

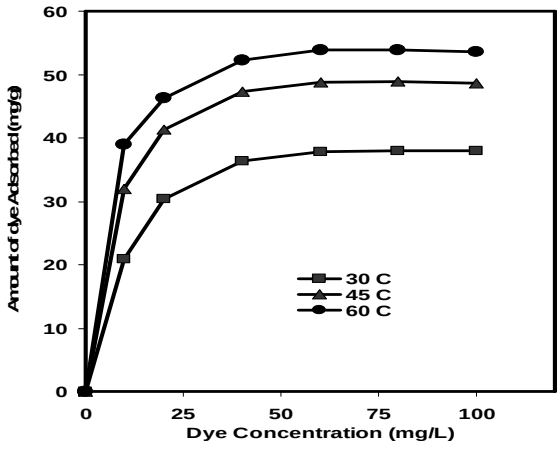

Fig. 8. Effect of specific dye uptake at different temperatures with methylene dye concentration.

Adsorption Isotherm

In general, an experimental isotherm is beneficial for defining adsorption capacity, facilitating the evolution of the process feasibility for a given application, selecting the most suited adsorbent, and determining the adsorbent dose needs. The Langmuir isotherm is the most common way to depict adsorption data from a solution. The isotherm experiment was carried out to achieve the best possible results. The Langmuir isotherm assumes that adsorption occurs in homogenous sites, that all sites are comparable, and that there are no interactions between the adsorbate molecule and neighbouring sites. The adsorption data were examined using the Langmuir isotherm equation in its linear version. The Langmuir isotherm equation of the following linearized form was applied to the sorption equilibrium at varied adsorbent dosages to determine the maximum adsorption capacity. The equation that describes the isotherm is as follows: (Eq-2 Type-I to IV). Where C_e represents the equilibrium dye concentration in solution (mg/L), q_e is the adsorption capacities (amount of dye adsorbed per weight of adsorbent,mg/g) K_L, and q_m are Langmuir constant that can be determined from above Langmuir linear equitation Type-I. A graph of q_e/C_e vs C_e was plotted. The constant K_L and q_m can be evaluated from the intercept and slope of this linear plot as shown in fig.9. Also, by comparing the correlation coefficient (R^2 value) shown in the table.2, the Langmuir isotherm model obtained a better fit of the experiment data.

A plot of the Langmuir isotherm Type II-IV $1/q_e$ versus $1/C_e$–Type II, q_e Vs q_e/C_e–Type III q_e/C_e Vs q_e–Type IV) Different dosages (1.0, 2.0, and 3.0g/L), pH (5.3, 6.9 and7.6) and Temperature (30, 45 and 60°C) as shown in fig.10-20, produced a linear graphical relationship in Table 2-3 that demonstrated the applicability of the aforementioned approach. The Langmuir linear equitation II and IV model is greater than zero but less than 1 (R^2) and this means that the process of the isotherms is favourable. The values obtained for Langmuir II and IV are similar to the result obtained by (Okafar *et al.,* 2012). Comparing the Langmuir coefficients of determination (R^2) values between the four different Langmuir models used, Langmuir II to IV has the highest value (0.9994), which means its better fitted than others.

The R^2 values of the Langmuir isotherm model when compared with other isotherm models. When a dye-containing solution and a powdered solid adsorbent material come into contact, the dyes first move from the bulk solution to the surface of the liquid film. A diffusion barrier is created by this surface. According to (Gupta et al., 2005), this barrier may be quite large or (Karthikesan *et al.,* 2010). The presence of a sizable amount of a diffusion barrier shows how film diffusion dominates the adsorption process. Additionally, external diffusion, internal diffusion, or a combination of both types of diffusions might affect how quickly an adsorption process moves forward. The solute species migration from the solution to the liquid phase's boundary layer is controlled by external diffusion. Internal diffusion, on the other hand, regulates the movement of the solute species from the adsorbent's exterior surface to its interior surface, or its pores (Karthikeyan *et al.,* 2010; Gupta *et al.,* 2003). It is now widely accepted that the dye adsorption process over a porous adsorbent involved the following three sequential phases (Crank, 1975; Karthikeyen *et al.,* 2010). Transport of the adsorbate ions to the adsorbent's external surface (film diffusion); (ii) Transport of the adsorbate ions within the adsorbent's pores, except for a small amount of adsorption that takes place on the external surface; and (iii) Adsorption of the incoming adsorbate ions on the adsorbent's interior surface.

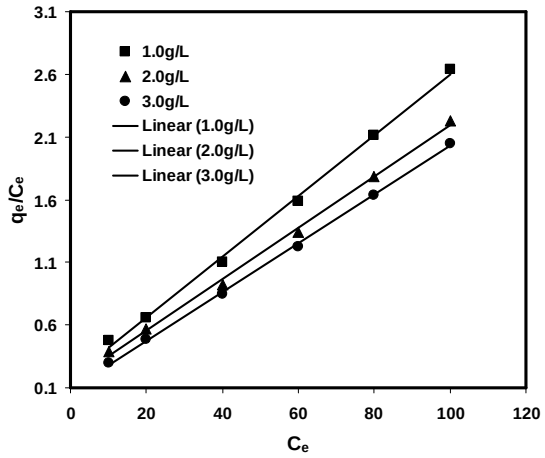

Fig. 9. Langmuir isotherm for the adsorption of Methylene blue dye using chitosan nanoparticle with orange peel Nanocomposite (Type-I).

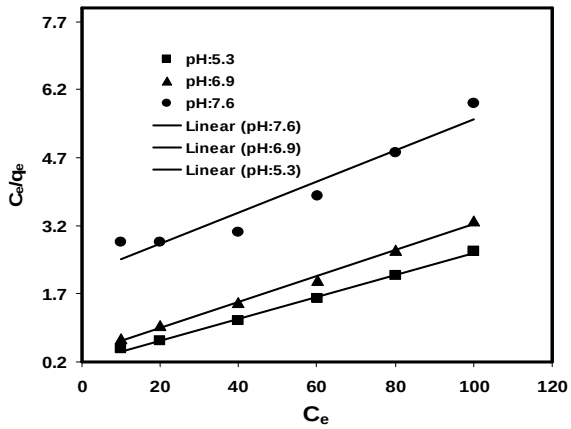

Fig. 10. Langmuir isotherm for the adsorption of Methylene blue dye using chitosan nanoparticle with orange peel Nanocomposite (Type-I).

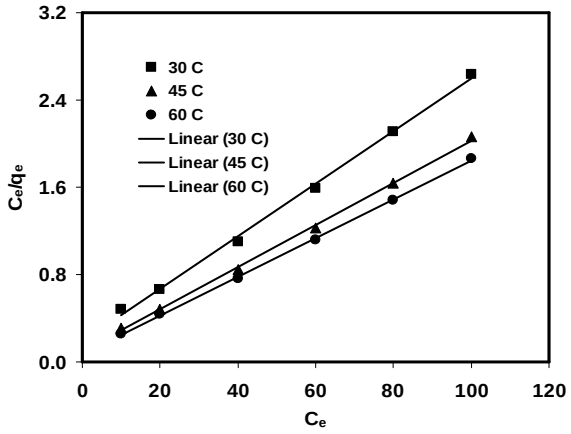

Fig. 11. Langmuir isotherm for the adsorption of Methylene blue dye using chitosan nanoparticle with orange peel Nanocomposite (Type-I).

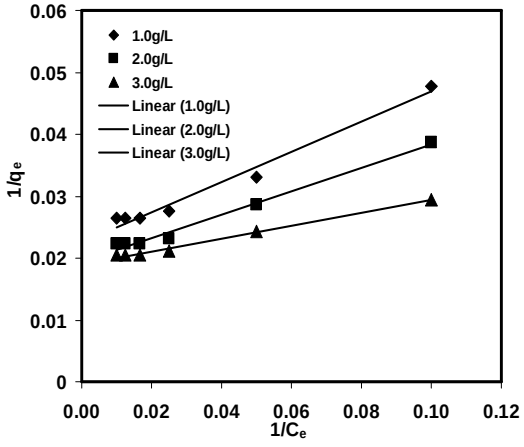

Fig. 12. Langmuir isotherm for the adsorption of Methylene blue dye using chitosan nanoparticle with orange peel Nanocomposite (Type-II).

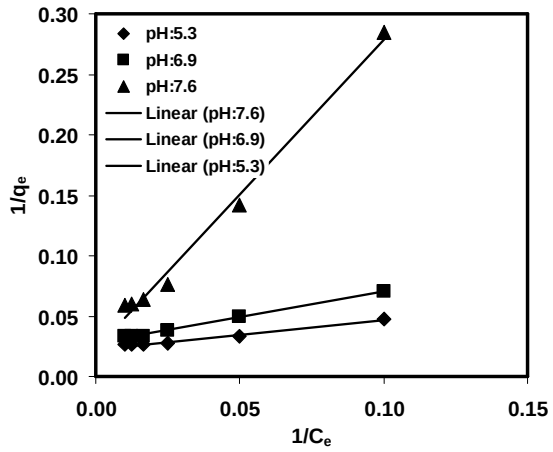

Fig. 13. Langmuir isotherm for the adsorption of Methylene blue dye using chitosan nanoparticle with orange peel Nanocomposite (Type-II).

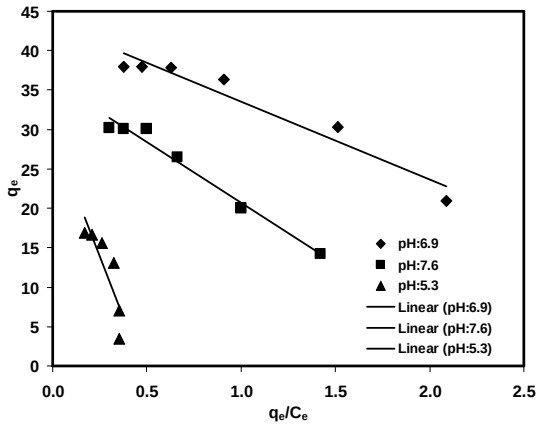

Fig. 16. Langmuir isotherm for the adsorption of Methylene blue dye using chitosan nanoparticle with orange peel Nanocomposite (Type-III).

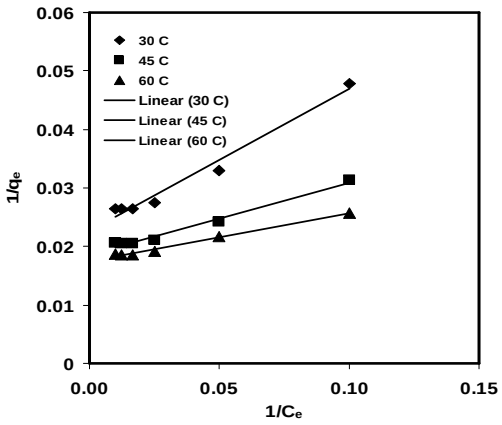

Fig. 14. Langmuir isotherm for the adsorption of Methylene blue dye using chitosan nanoparticle with orange peel Nanocomposite (Type-II).

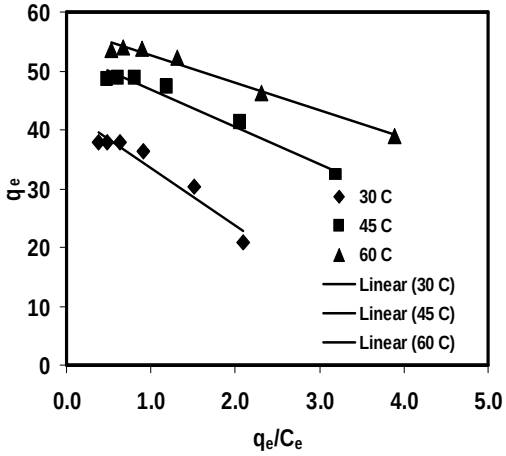

Fig. 17. Langmuir isotherm for the adsorption of Methylene blue dye using chitosan nanoparticle with orange peel Nanocomposite (Type-III).

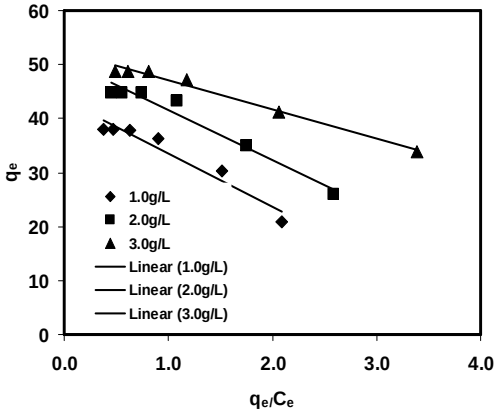

Fig. 15. Langmuir isotherm for the adsorption of Methylene blue dye using chitosan nanoparticle with orange peel Nanocomposite (Type-III).

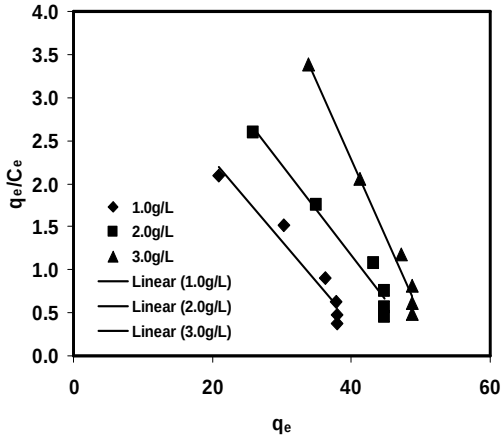

Fig. 18. Langmuir isotherm for the adsorption of Methylene blue dye using chitosan nanoparticle with orange peel Nanocomposite (Type-IV).

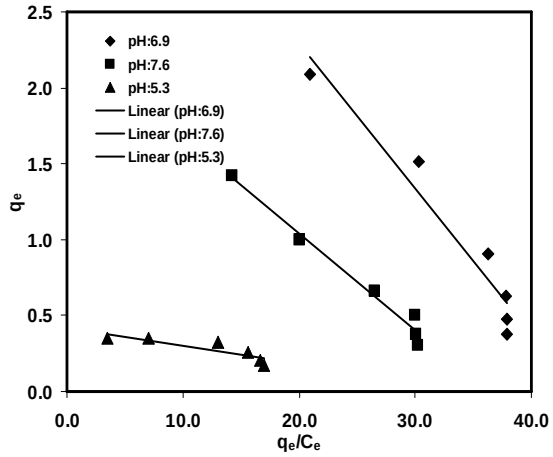

Fig. 19. Langmuir isotherm for the adsorption of Methylene blue dye using chitosan nanoparticle with orange peel Nanocomposite (Type-IV).

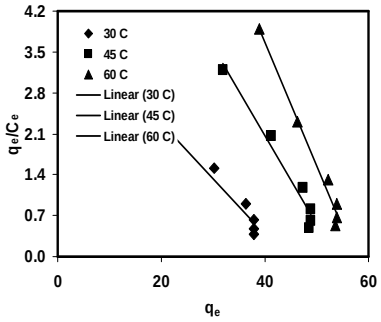

Fig. 20. Langmuir isotherm for the adsorption of Methylene blue dye using chitosan nanoparticle with orange peel Nanocomposite (Type-IV).

The heterogeneous surface energies system is used by Equation (3) (Freundlich *et al.,* 1906). The sorption isotherm is the most convenient form of representing the experimental data at different adsorbent dosages, temperatures, and pH as shown in Fig. 21-23. Freundlich isotherm model was also used to explain the observed phenomenon. The Freundlich isotherm, Where, Ce is the equilibrium concentration (mg/l), X is the amount of dye removal (mg), m is the weight of the adsorbent used (g), and K_f and n are constantly incorporating all factors affecting the adsorption process such as adsorption capacity and intensity, they adsorption follows Freundlich isotherm model (Dosages, pH and temperature) as well (fig.21-23). K_f and n were calculated from the intercept and slope of the plots. According to (Treyball, 1980), it has been shown using mathematical calculations that n was between 1 and 10 representing beneficial adsorption. The various constants, associated with the isotherm are the intercept, which is roughly an indicator of sorption capacity (k_f) and the slope (n) sorption intensity values are recorded in fig.21-23. The values n>1 represent favourable adsorption conditions. In most of the cases the exponent between 1<n<10 shows the beneficial adsorption as shown in Table 1.

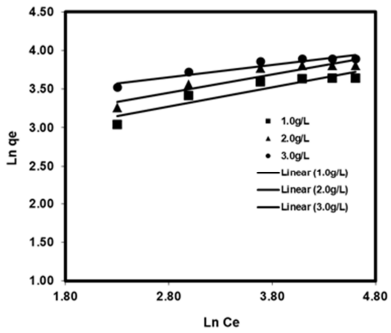

Fig. 21. Freundlich isotherm for the adsorption of Methylene blue dye using chitosan nanoparticle with orange peel Nanocomposite.

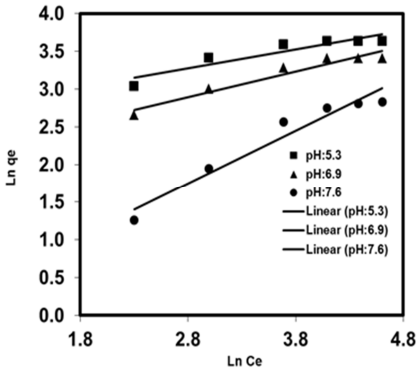

Fig. 22. Freundlich isotherm for the adsorption of Methylene blue dye using chitosan nanoparticle with orange peel Nanocomposite.

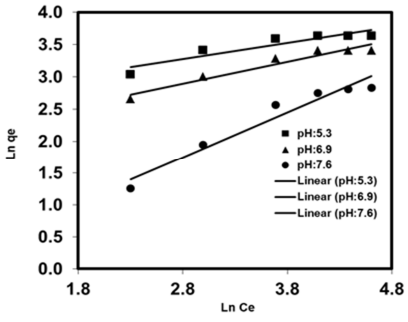

Fig. 23. Freundlich isotherm for the adsorption of Methylene blue dye using chitosan nanoparticle with orange peel Nanocomposite

Table 2. Langmuir and Freundlich isotherm constants at different adsorbent dosages, Temperatures, and pH. (Chitosan nanoparticle with orange peel Nanocomposite – Methylene blue dye).

Parameters		Langmuir Isotherm -model parameters	Freundlich Isotherm -model parameters
		TYPE I	
Dosage (g/ L)	1.0	K_L=0.13; q_m=41.49; R^2=0.9970	K_f=2.257; n=4.006; R^2=0.869
	2.0	K_L=0.14; q_m=48.78; R^2=0.9978	K_f=2.791; n=4.215; R^2=0.883
	3.0	K_L =0.22; q_m=51.55; R^2=0.9994	K_f=3.209; n=6.305; R^2=0.897
Temperature (°C)	30	K_L =0.13; q_m=41.49; R^2=0.9975	K_f=2.572; n=0.388; R^2=0.859
	45	K_L =0.21; q_m=51.55; R^2=0.9988	K_f=3.126; n=0.319; R^2=0.863
	60	K_L =0.27; q_m=56.18; R^2=0.9993	K_f=3.385; n=0.295; R^2=0.891
pH	5.3	K_L =0.02; q_m=29.07; R^2=0.9269	K_f=2.572; n=0.388; R^2=0.859
	6.9	K_L =0.07; q_m=35.09; R^2=0.9963	K_f=1.949; n=0.513; R^2=0.939
	7.6	K_L =0.13; q_m=41.49; R^2=0.9975	K_f=0.209; n=4.782; R^2=0.946

Table 3. Langmuir isotherm constants at different Dosages, pH, and Temperatures (chitosan nanoparticle with orange peel Nanocomposite – Methylene blue – Type - II).

Parameters		Langmuir Isotherm -model
		TYPE II
Dosage (g/ L)	1.0	K_L = 0.093; q_m = 44.24; R^2= 0.9789
	2.0	K_L = 1.039; q_m= 5.128; R^2= 0.9883
	3.0	K_L = 0.105; q_m= 90.90; R^2 = 0.9927
Temperature (°C)	30	K_L = 0.093; q_m= 44.24; R^2= 0.9789
	45	K_L = 0.213; q_m= 57.14; R^2= 0.9909
	60	K_L = 1.510; q_m= 53.76; R^2= 0.9848
pH	5.3	K_L = 0.009; q_m= 43.29; R^2= 0.9912
	6.9	K_L = 0.064; q_m= 36.23; R^2= 0.9956
	7.6	K_L = 0.093; q_m= 44.24; R^2= 0.9789

Table 4. Langmuir isotherm constants at different Dosages, pH, and Temperatures (chitosan nanoparticle with orange peel Nanocomposite – Methylene blue dye – Type - III).

Parameters		Langmuir Isotherm -model
		TYPE III
Dosage (g/ L)	1.0	K_L = 0.101; q_m = 43.361; R^2 = 0.9370
	2.0	K_L = 0.108; q_m = 50.767; R^2 = 0.9610
	3.0	K_L = 0.184; q_m = 52.481; R^2 = 0.9830
Temperature (°C)	30	K_L = 0.101; q_m = 43.36; R^2 = 0.9370
	45	K_L = 0.157; q_m = 53.29; R^2 = 0.9650
	60	K_L = 0.215; q_m = 57.24; R^2 = 0.9810
pH	5.3	K_L = 0.016; q_m = 29.32; R^2 = 0.9830
	6.9	K_L = 0.101; q_m = 43.36; R^2 = 0.9370
	7.6	K_L = 0.064; q_m = 36.10; R^2 = 0.9610

Table 5. Langmuir constants at different Dosages, pH, and Temperatures (chitosan nanoparticle with orange peel Nanocomposite - Methylene blue dye – Type - IV).

Parameters		Langmuir Isotherm -model
		TYPE IV
Dosage (g/ L)	1.0	K_L = 0.095; q_m = 44.010; R^2= 0.9370
	2.0	K_L = 0.104; q_m = 55.104; R^2= 0.9610
	3.0	K_L = 0.189; q_m = 50.419; R^2= 0.9830
Temperature (°C)	30	K_L = 0.095; q_m = 44.010; R^2= 0.9370
	45	K_L = 0.152; q_m = 53.605; R^2= 0.9650
	60	K_L = 0.211; q_m = 57.368; R^2= 0.9810
pH	5.3	K_L = 0.063; q_m = 36.34; R^2= 0.9760
	6.9	K_L = 0.011; q_m = 35.45; R^2= 0.7360
	7.6	K_L = 0.095; q_m = 44.010; R^2= 0.9370

Conclusions

The removal of various colours from textile wastewater by adsorption on chitosan nanoparticles with orange peel nanocomposite has been proven to be useful for decreasing water pollution caused by dyes, according to this study.

Chitosan nanoparticles with orange peel nanocomposite can be utilized as an adsorbent if it is abandoned as garbage from a fruit stand. The hydrothermal technique was used to modify the orange peel to generate Chitosan nanoparticles in situ. SEM, FTIR, and TGA analysis were used to analyze the orange peel, chitosan with orange peel, chitosan nanoparticle, and chitosan nanoparticle with orange peel nanocomposite. SEM, FTIR, and TGA were used to confirm the existence of chitosan nanoparticles in orange peel nanocomposite. FT-IR research revealed a shift in the functional groups of orange peel during the production of chitosan nanoparticles. Based on the findings, the orange peel can be used as a soft cellulose material in conjunction with polymer matrices to fabricate green composites in high-temperature and adsorption experiments. Chemists and scientists, in general, are constantly looking for ways to decrease these contaminants. The removal of these toxins would promote healthy living and provide mankind with a slew of good news. Human health is jeopardized by the presence of these dyes in aquatic systems. As a result, removing such colours from water bodies could be a fascinating and essential study project. This research demonstrates that orange peel-modified chitosan can be employed as an effective adsorbent for removing methylene blue dye from solutions. In the Langmuir and Freundlich isotherm models, chitosan nanoparticle with orange peel nanocomposite fits better for the adsorption of methylene blue dye, and the reaction is endothermic as well spontaneous and practicable, according to this study. Chitosan nanoparticle with orange peel nanocomposite is regarded as a good adsorbent for removing methylene blue dye from aqueous solutions. As a result, it should be used to remove colours from the environment because it is readily available and inexpensive. The experimental data acquired in this study can be used to build and optimize a cost-effective dye removal technique for industrial effluents.

References

Acemioglu B. 2004. Adsorption of Congo red from aqueous solution onto calcium-rich fly ash, J. Colloid Interf. Sci. **274,** 371-379.

Al-Qodah Z. 2000. Adsorption of dyes using shale oil ash, Water Res. **34,** 4295-4303.

Arthanarieswaran VP, Kumaravel A, Saravanakumar S. 2015. Physico-Chemical properties of Alkali Treated *Acacia leucophloea* Fibers. International Journal of Polymer Analysis and Characterization **20(8),** 704-13.

Arulmozhi KT, Mythili N. 2013. Studies on the chemical synthesis and characterization of lead oxide nanoparticles with different organic capping agents AIP advances **3,** 122.

Ashok B, Obi Reddy K, Krittirash Yorseng, Rajini N, Hariram N, Varada Rajulu A. 2018. Modification of Natural Fibers from *Thespesia lampas* Plant by in Situ Generation of Silver Nanoparticles in Single-Step Hydrothermal Method. International Journal of Polymer Analysis and Characterization **23(6),** 509-16.

Chen BCW, Hui G, McKay, Langmuir. 2007. 17 (2001) 740. Colloids and Surfaces A: Physicochem. Eng. Aspects **299,** 232-238.

Crank J. 1975. The Mathematics of Diffusion, Clarendon, Oxford **(2nd Ed)**.

Dizge N, Kara S, Aydiner C, Demirbas E, Kobya M. 2008. Adsorption of reactive dyes from aqueous solutions by fly ash: Kinetic and equilibrium studies. Journal of Hazardous Materials **150(3),** 737-746.

Freundlich HF. 1906. Uber die adsorption in losungen, Zeitschrift Physikalische Chemie **57,** 385-470.

Gomathi T, Prasad S, Sudha PN, Sukumaran A. Size optimization and in vitro biocompatibility studies of chitosan nanoparticles. Int J. Biol. Macromol **104,** 1794-1806

Gordon Mckay, Stephen J, Allen. 1980. Can Surface mass transfer processes using peat as an adsorbent for dyestuffs. J. Chem. Eng **58,** 521 -526.

Gordon McKay, Michael S, Otterburn, Jamal A, Aga. 1985. Fuller's earth and fired clay as adsorbents for dyestuffs Equilibrium and rate studies. Water, Air and Soil Pollution **24,** 307-322.

Gupta VK, Ali I, Suhas, Mohan D. 2003. Equilibrium uptake and sorption dynamics for the removal of a basic dye (basic red) using low-cost adsorbents. J. Colloid Interface Sci **265,** 257-264.

Gupta VK, Mittal A, Gajbe V. 2005. Adsorption and desorption studies of a water-soluble dye, Quinoline Yellow, using waste materials. J. Colloid Interface Sci. **284,** 89-98.

Hafsa J, Ali Smach M, Khedher MRB, Charfeddine B, Limem K, Majdoub H, Rouatbi S. 2016. Physical, antioxidant and antimicrobial properties of chitosan films containing *Eucalyptus globulus* essential oil. LWT-Food Science and Technology **68,** 356-364.

Ho YS, McKay G. 1999. A kinetic study of dye sorption by biosorbent waste product pith. Res Conserv Recycling **25,** 171-193.

Janos P, Buchtova H, Ryznarova M. 2003. Sorption of dyes from aqueous solutions onto fly ash, Water Res. **37,** 4938-4944.

Karthikesan K, Pari L, Menon VP. 2010. Antihyperlipidemic effect of chlorogenic acid and tetrahydrocurcumin in rats subjected to diabetogenic agents. Chem. Biol. Interact **188(3),** 643-650.

Karthikeyan S, Sivakumar B, Sivakumar N. 2010. Film and Pore Diffusion Modeling for Adsorption of Reactive Red 2 from Aqueous Solution on to Activated Carbon Prepared from Bio-Diesel Industrial Waste. E-Journal of Chemistry **7(1),** 175-184.

Khan A, Asiri AM, Aslam Parwaz Khan A, Sirajuddin & Gupta V. 2015. Room temperature preparation, electrical conductivity and thermal behavior evaluation on silver nanoparticle embedded polyaniline tungstophosphate nanocomposite. Polymer Composites **37(8),** 2460-2466.

Li G, Zhao XS, Madhumita BR. 2007. Advanced oxidation of orange-II using TiO_2 supported on porous adsorbents: The role of pH, H_2O_2 and O_3. Separation and Purification Technology **55,** 91-97.

Li P, Xia J, Shan Y, Niel Z, Wang F. 2015. Effects of surfactants and microwave-assisted pretreatment of orange peel on extracellular enzymes production by *Aspergillus japonicas*. Appl. Biochem. Biotechnol. **176,** 758-771.

Li Jinyang, Jinming Zhang, Hariram Natarajan, Jun Zhang, Basa Ashok. 2019. Modification of Agricultural Waste Tamarind Fruit Shell Powder by in Situ Generation of Silver Nanoparticles for Antibacterial Filler Applications. International Journal of Polymer Analysis and Characterization **24(5),** 421-27.

Lopez-Velazquez MA, Santes V, Balmaseda J, Torres-García E. 2013. Pyrolysis of orange waste: A thermo-kinetic study. J. Anal. Appl. Pyrol. **99,** 170-177.

Mafra MR, Mafra L, Zuim DR, Vasques EC, Ferreira MA. 2013. Adsorption of remazol brilliant blue on an orange peel adsorbent. Braz. J. Chem. Eng. **30,** 657-665.

McKay G, Ramprasad P, Mowli. 1986. Equilibrium studies for the adsorption of dyestuffs from aqueous solutions by low-cost materials. Water Air Soil Pollut. **29,** 273.

Mohan D, Singh KP, Singh G, Kumar K. 2002. Removal of dyes from wastewater using fly ash, A low-cost adsorbent, Ind. Eng. Chem. Res. **41,** 3688-3695.

Namasivayam C, Kavitha D. 2002. Removal of Congo Red from water by adsorption onto activated carbon prepared from coir pith, an agricultural solid waste, Dyes and Pigments **54,** 47-58.

Namasivayam C, Kanchana N, Yamuna RT. 1993. Waste banana pith as adsorbent for the removal of rhodamine-B from aqueous solution. Waste Management **19,** 89.

Namasivayam C, Kanchana N. 1992. Waste banana pith as adsorbent for color removal from wastewaters. Chemosphere **25(11),** 1691-1705.

Namasivayam C, Radhika R, Subha S. 2001. Uptake of dyes by a promising locally available agricultural solid waste: Coir pith. Waste Manage**,** **38,** 381-387.

Namasivayam C, Ranganathan K. 1997. Removal of congo red from wastewater by adsorption onto waste red mud. Chemosphere **34(2),** 401-417.

Namasivayam C, Yamuna RT. 1994. Utilizing biogas residual slurry for dye adsorption. Amer Dye Stu Rep **83,** 22.

Namasivayam N, Muniasamy K, Gayathri M, Rani K, Ranganathan. 1996. Removal of dyes from aqueous solutions by cellulosic waste orange peel, Biores. Technol **57,** 37.

Neill C, Hawkes FR, Hawkes DL, Lourenco N, Pinheiro HM, Delee W. 1999. Colour in textile effluents- sources, measurement, discharge consents, and simulation: A review, J. Chem. Technol. Biotechnol. **74,** 1009-1018.

Netpradit S, owprayoon ST. 2003. Application of 'waste' metal hydroxide sludge for adsorption of Azo reactive dyes. Water Res **37,** 763 -772.

Okafor PC, Okon PU, Daniel EF, Ebenso E. 2012. Int. J. Electrochem. Sci **7,** 12354–12369.

Sugumaran P, Priya V, Susan P, Ravichandran and Seshadri S. 2012. Production and Characterization of Activated Carbon from Banana Empty Fruit Bunch and Delonix regia Fruit Pod. Journal of Sustainable Energy & Environment **(3)**, 125-132.

Rahman MM, Khan A, Asiri AM. 2015. Chemical sensor development based on poly (o-anisidine) silverized-MWCNT nanocomposites deposited on glassy carbon electrodes for environmental remediation. RSC Advances **5(87),** 71370-71378.

Saini J, Garg VK, Gupta RK. 2018. Removal of Methylene Blue from aqueous solution by Fe3O4@Ag/SiO2 nanospheres: synthesis, characterization and adsorption performance. J. Mol. Liq. **250,** 413-422.

Santhanam K, Kumaravel A, Saravanakumar S, Arthanarieswaran VP. 2016. Characterization of New Natural Cellulosic Fiber from *Ipomoea* Staphylinaplant. International Journal of Polymer Analysis and Characterization **21(3),** 267-74.

Slokar YM, Le Marechal AM. 1997. Methods of decolouration of textile wastewaters, Dyes Pig **37,** 335-356.

Sugumar S, Mukherjee A, Chandrasekaran N. 2015. Eucalyptus oil nanoemulsion-impregnated chitosan film: Antibacterial effects against a clinical pathogen, *Staphylococcus aureus*, *in vitro*. International Journal of Nanomedicine **10(Suppl 1),** 67-75.

Sun Kou MR, Mendioroz S, Guijarro MI. 1998. A thermal study of Zr-pillared montmorillonite, J. Thermochim. Acta **323 (1-2),** 145-157.

Sung AK, Park K, DoKim H, Taik K. 2002. Preparation of silica nanoparticles: Determination of the optimal synthesis conditions for small and uniform particles. Colloids and Surfaces A: Physicochemical and Engineering Aspects 197(1-3), 7-17.

Thio Christine Chandra, Magdalena Maria Mirna, Jaka Sunarso, Yohanes Sudaryanto, SuryadiIsmadji. 2009. Activated carbon from durian shell: Preparation and characterization. Journal of the Taiwan Institute of Chemical Engineers **40(4),** 457-462.

Treyball RE. 1980. Mass transfer operations. **3rd Ed**. New York: McGraw Hill.

Tverdokhlebov, Sergei I, Viktor P, Ignatov, Igor B, Stepanov, Denis O Sivin, Danila G, Petlin. 2012. Hybrid method for the formation of biocomposites on the surface of stainless-steel implants, Engineering **4,** 613-618.

Viraraghavan T, Ramakrishna K R. 1999. Fly ash for color removal from synthetic dye solutions, Water Qual. Res. J. Can. **34** 505-517.

Yoo JH, Lee HB, Choi SW, Kim YB, Sumathy B, Kim EK. 2011. Production of an antimicrobial compound by Bacillus subtilis LS 1–2 using a citrus-processing by-product. Korean J. Chem. Eng **28,** 1400-1405.

Yunus Alparslan, Taçnur Baygar. 2017. Effect of Chitosan Film Coating Combined with Orange Peel Essential Oil on the Shelf Life of Deepwater Pink Shrimp. Food Bioprocess Technology **10,** 842-853.

Zollinger H. 1987. Color Chemistry: Synthesis, Properties and Applications of Organic Dyes and Pigments. **1st Edition,** Weinheim, New York.